Triaxial Tests to Assess the Effects of Densification, Lateral Spreading and Grain Breakage on Settlement Behaviour of Full-Size Railway Ballast

Rashid S. Abeid, Madhusudan B. N. Murthy, Taufan Abadi, David Milne, Joel Smethurst, and William Powrie

Abstract Predicting the rate of deterioration of ballasted track due to cumulative plastic settlement is a major challenge for railway infrastructure owners. For track on a stiff subgrade, more than 50% of the total deformation originates from the ballast through grain rearrangement (compaction), lateral spreading and possibly grain breakage. Despite much research, knowledge of the mechanisms by and extent to which these three processes contribute to permanent settlement is limited, and permanent settlement is still usually estimated empirically. This paper describes the rationale and initial results of triaxial tests on full-size granite railway ballast, carried out to investigate the relative importance of the processes responsible for ballast settlement. Specimens of full-size railway ballast 600 mm high and 300 mm in diameter were subjected to cycles of deviator stress between 10 kPa and 50, 100 or 200 kPa. Tests were carried out over up to 500,000 load cycles at a frequency of 3 Hz and an effective confining stress (cell pressure) of 30 kPa. For the ballast tested, grain rearrangement and lateral spreading were the dominant effects on the evolution of ballast permanent settlement. Grain breakage was insignificant except at the highest test load.

Keywords Ballast · Settlement · Breakage · Rearrangement · Lateral spreading

1 Introduction and Background

Railway track geometry must remain within strict limits of deviation from the desired line and level, for reasons of passenger comfort and operational safety. Differential permanent settlement has always been a concern for the railway sector as the situation leads to track misalignment. For track on a stiff subgrade, more than 50% of

R. S. Abeid (✉) · M. B. N. Murthy · T. Abadi · D. Milne · J. Smethurst · W. Powrie
University of Southampton, Boldrewood Innovation Campus, Southampton SO16 7QF, UK
e-mail: r.s.abeid@soton.ac.uk

C. Rujikiatkamjorn et al. (eds.), *Proceedings of the 5th International Conference on Transportation Geotechnics (ICTG) 2024, Volume 6*, Lecture Notes in Civil Engineering 407, https://doi.org/10.1007/978-981-97-8233-8_25

the total deformation originates from the ballast [1] through grain rearrangement (compaction), lateral spreading and possibly grain breakage. This article investigates the extent to which these three processes contribute to permanent settlement at different loads, by means of triaxial tests on specimens of full-size railway ballast.

Ballast settlement is generally held to occur in different phases. Each phase is associated with different rates but the mechanisms responsible remain a matter of conjecture [2]. Experiments on various ballast materials have shown that the permanent settlement develops initially quite rapidly, but after several thousands of load cycles becomes slower [2–4]. The initial rapid deformation is mainly attributed to the compaction of the ballast through grain rearrangement, which reduces the volume of inter-granular voids. Lateral spreading is also likely, although this might reduce with ballast densification and the development of a shallower (hence more stable) slope. The importance of grain breakage would be expected to depend on the mineralogy; grain size, shape and mechanical properties (strength and toughness); the nature of the contacts; and the magnitude of the load to which the ballast is subjected.

Densification (compaction) through grain rearrangement is generally considered to be the main cause of a large rate of settlement at the beginning of loading. The potential for further compaction reduces as the ballast densifies. Maintenance tamping may loosen the ballast, causing the initial high rate of settlement to be repeated [1, 6].

In most railways the ballast is elevated above the adjacent ground and the resulting shoulder slope is not confined. Hence vertical loading of the track causes the ballast to spread laterally. The rate of lateral spreading may decrease with the number of loading cycles if a more stable ballast shoulder slope geometry is allowed to develop. Also, lateral spreading can be reduced by reducing the slope of the ballast shoulder [4, 7]. Heaping the ballast above the level of the sleeper top is beneficial in increasing the lateral resistance [8, 9], but this is separate from (and not to be confused with) a shoulder that slopes downward below the level of the sleeper.

Breakage of ballast grains into smaller fragments may contribute to the settlement of a railway trackbed. It may involve the attrition of grains, corner breakage and grain splitting [10]. The newly generated finer particles resulting from breakage can occupy the voids in the original structure, leading to a decrease in the overall and specific volume. Several factors may influence grain breakage including:

i. *Mineralogy*. A high-quality ballast should be made from rock with a high specific gravity, shear strength, toughness, hardness and resistance to weathering [11, 12]. In the United Kingdom (UK), granite is now widely used especially on principal routes, although in the past other minerals (especially limestone) were common. Experiential evidence of ballast behaviour must therefore be treated with a degree of caution, as it may relate to minerals historically but not currently used.
ii. *Angularity of the grains*. Angular grains are more susceptible to corner breakage than less angular grains. In triaxial tests by [13], most of the corner breakage occurred during the first 1000 loading cycles. However, this may not impair the performance of the ballast; work by [14, 15] showed that the reused (recovered

and cleaned) ballast does not behave significantly differently from fresh ballast of similar mineralogy.

iii. *Grain size*. It was observed by [16] in triaxial tests on 19–53 mm aggregates that larger grains were more susceptible to breakage than smaller grains of the same mineralogy. This is because the larger grains are more likely to contain weaknesses that have already fractured in the creation of the smaller grains.

iv. *Tamping*. Maintenance tamping aims to restore the track geometry following differential settlement. However, the process has a detrimental effect due to breakage and attrition of ballast grains [11, 17–19].

v. *Load amplitude*. Ballast grains are more susceptible to breakage when subjected to higher loads [20, 21]. This is also demonstrated in the results presented in this paper.

vi. *Loading frequency*. According to [13, 22] more breakage occurs at higher frequencies than at lower frequencies. However, at high frequencies and amplitudes the accelerations can be large, and it is important to consider appropriate values of these parameters when choosing laboratory test loads intended to represent those in the field [23].

2 Materials and Methods

The experiments were conducted in a large triaxial apparatus on specimens 600 mm in height and 300 mm in diameter (Fig. 1). Granite ballast from the Mountsorrel quarry in Leicestershire, UK with a grain size distribution conforming to the Network Rail standard was used. Tests on three different specimens were conducted, all at a cell pressure of 30 kPa. A conventional 2.5 m long × 0.29 m wide G44 sleeper loaded by 50% of a 25 tonne (250 kN) axle will exert vertical stress, averaged over the whole of the sleeper area, of 172 kPa. Assuming a horizontal stress of $\left(1 - \sin\phi'\right)$ times the vertical effective stress with $\phi = 45°$ gives a horizontal effective stress of about 50 kPa. Although in principle the horizontal effective stress should increase in proportion to the vertical, this adds to the complexity of the testing regime and when attempted can give counter-intuitive results [6]. Hence, for simplicity, the cell pressure for the tests reported in this paper was kept constant at 30 kPa while cyclic deviator stresses up to maxima of 50, 100 and 200 kPa were applied.

Hundreds of thousands of load cycles were applied at a frequency of 3 Hz. Although this corresponds approximately to the fundamental vehicle passing frequency of a train formed of cars 23 m in length travelling at 252 km/hour, in reality train passage subjects the track to a series of sinusoidal loads of different magnitudes at multiples of up to about ten times the car passing frequency. Hence the test frequency does not, and was not intended to, represent any real loading frequency or train speed, rather, it was chosen as it was slow enough not to over-excite the test apparatus while enabling the tests to be completed within a reasonable timeframe. Specimens were initially loose, with an as-placed density ranging from 1450 to 1506 kg/m^3. The deviator stress was cycled between a minimum value of

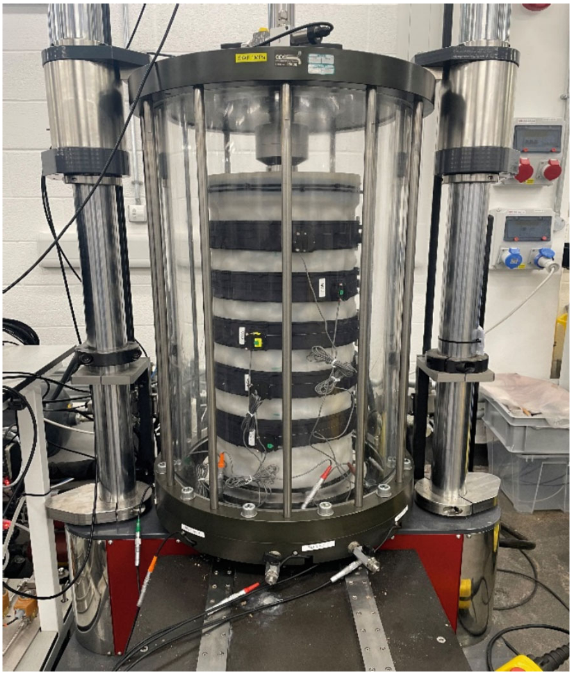

Fig. 1 Triaxial set-up with 5 radial belts

10 kPa and the notional maxima q_{max} indicated in Table 1. The test was controlled by specifying the equivalent ram load, based on the initial (undeformed) specimen area; this led to some variability in the actual deviator stress achieved, as indicated in the results presented.

Once the specimen had been placed within the apparatus and the cell pressure applied, the loading ram was brought into contact with the top cap and a small "docking load" of 1.4 kPa applied. This was to ensure positive contact while avoiding unwanted deformation prior to testing. Then all the measurements were set to zero and the load was increased to the datum (midpoint) value, from which the test commenced.

Output data were recorded at a frequency of 60 Hz (20 data points per cycle) to prevent aliasing. Five equally-spaced radial belts were used to track the change in circumference of the sample. Two sensors within the load cell were used to measure

Table 1 Data for triaxial tests at 3 Hz and 30 kPa of confining pressure

Test ID	q_{max} (kPa)	q_{min} (kPa)	Datum stress (kPa)	Initial density (kg/m^3)	Number of load cycles	Cell pressure (kPa)
Test 1	50	10	30	1506	250,000	30
Test 2	100	10	55	1450	500,000	30
Test 3	200	10	105	1466	250,000	30

Fig. 2 **a** Ballast sample used in test 3 (63 mm > Red > 50 mm > Yellow > 40 mm < Colourless < 31.5 mm < Green < 22.4 mm. **b** Test 3 sample before the test. **c** Test 3 sample after the test

the variations in cyclic load and axial displacement with time. Sieve tests were conducted before and after each test, and the results used to assess grain breakage. Grains in Test 3 were painted with Arco Heavy-Duty Line Marking paint to assist with this (Fig. 2).

3 Results and Discussion

The results of the three tests are summarized in Table 2 and Figs. 3, 4 and 5. The axial displacement, lateral spreading and densification or dilation of the sample are indicated by the graphs of axial strain, radial strain and volumetric strain respectively in Figs. 3a, 4a and 5a. Figures 3b, 4b and 5b show the evolution of q/p' with number of load cycles.

In Test 1 (Fig. 3a), ballast settlement and volumetric strain were still ongoing at the end of the test, after 250,000 loading cycles. Lateral spread was minimal and grain breakage was undetectable. The small negative axial strain apparent over the first few cycles is a result of taking the strain datum at the mid-point of the first load cycle (at 30 kPa rather than at zero).

Table 2 Triaxial tests results at the end of each test

Test ID	Broken mass (g)	Broken mass (0/000)	Circumferential lateral spreading (mm)	Total axial displacement (mm)
Test 1	–	–	0	2.27
Test 2	3.45	0.56	0.88	12.18
Test 3	38.04	6.12	119.90	114.74

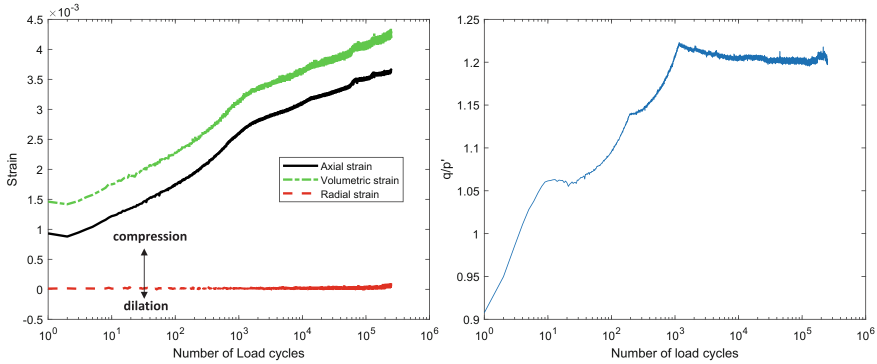

Fig. 3 **a** Axial, radial and volumetric strain versus number of load cycles for Test 1. **b** q/p' vs number of load cycles

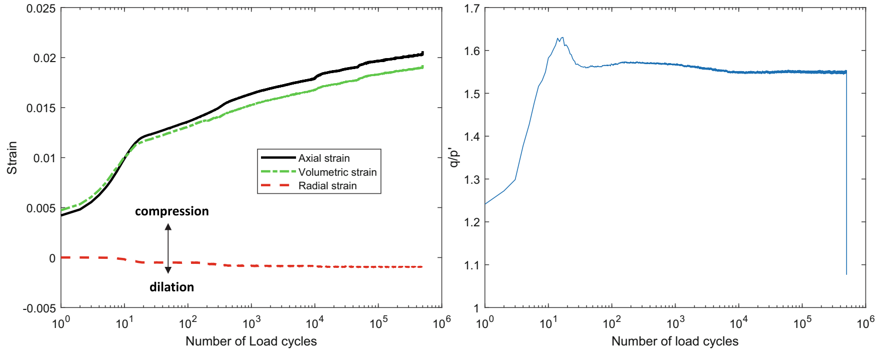

Fig. 4 **a** Axial, radial and volumetric strain versus number of load cycles for Test 2. **b** q/p' versus number of load cycles

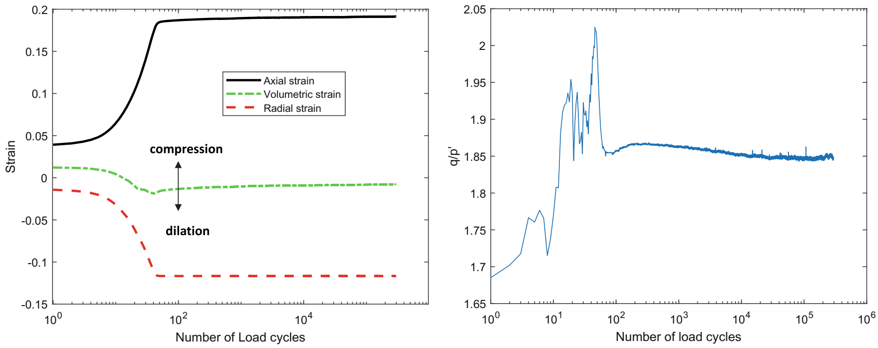

Fig. 5 **a** Axial, radial and volumetric strain versus number of load cycles for Test 3. **b** q/p' versus Number of load cycles

In Test 2 (Fig. 4a), lateral spreading was more significant than in Test 1 but still small. This is not altogether surprising as, relative to the vertical load, the lateral confining stress was smaller in Test 2 than in Test 1. Most of the vertical settlement is accounted for by volumetric change. Again, volumetric and axial strain were ongoing at the end of the test after 500,000 cycles. Grain breakage was detectable but small, with broken fragments accounting for 0.56 parts per 10,000 by mass (0.0056%) by the end of the test (an actual mass of 3.45 g). To ascertain when this breakage occurred, it would be necessary to carry out tests with progressively fewer loading cycles.

Figure 5a shows the result of Test 3, which are quite different from those of Test 1 and Test 2. The specimen to collapse between 10 and 45 cycles when the stress ratio q/p' increased from about 1.7 to the target value of 2. This was accompanied by substantial axial and radial strain (settlement and lateral spreading) but relatively little volumetric change (densification). After 45 load cycles the specimen dilated slightly and the axial and radial strains remained almost constant while the stress ratio q/p' cycled to a maximum, apparently stable, value of about 1.85. This suggests that the specimen may have failed, with the associated geometric distortion sufficient to enable cycling at a stable stress ratio up to a maximum value of q of about 160 kPa, with a small increase in radial stress (from 30 to 32 kPa) due to the stretching of the rubber membrane calculated according to [24] Method.

Grain breakage in Test 3 was much more significant than in either of the other tests, with a broken mass at the end of the test of 38.04 g (6.12 parts per 10,000 or 0.0612% by mass). Breakage occurred by surface flaking in addition to attrition/abrasion, and corner breakage/loss of asperities (Fig. 6). Grain splitting was insignificant.

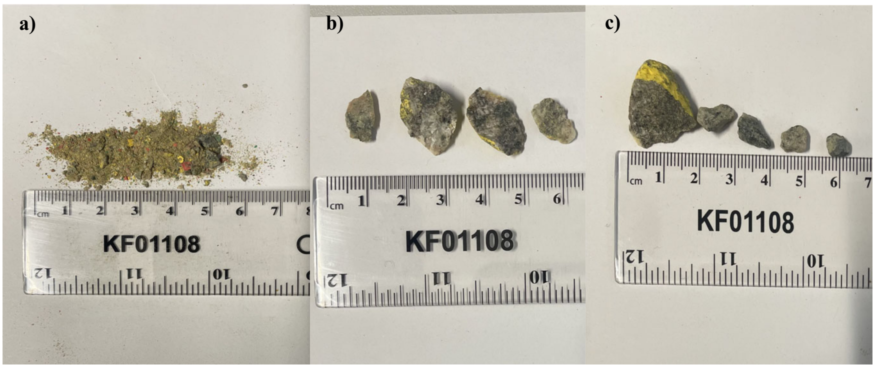

Fig. 6 Grain breakage by **a** Attrition/abrasion **b** Surface flaking **c** Corner breakage

4 Conclusions

1. The most significant driver of settlement at low and medium loads was densification. However, the lateral stress in these tests was proportionately higher than it would be in the field, especially at the sleeper end near a shoulder slope.
2. Lateral spread was only a factor at the highest vertical load (Test 3). In this test, the ballast appeared to fail to a geometry at which the applied deviatoric load could be supported over a greater area by means of a reduced stress.
3. Grain breakage is potentially much more significant at higher stresses. Breakage by surface flaking as well as attrition/abrasion and corner breakage was observed. It is not possible from the tests carried out to determine where the breakage occurred—for example prior to specimen failure, or progressively throughout the whole test. Further work is be needed to ascertain this.
4. Further testing is also needed to quantify the effects of initial density and lateral confining stress, including whether this should be cycled with the vertical stress so they remain proportionally similar.

References

1. Brown SF, Selig ET (1991) The design of pavement and rail track foundations, cyclic loading of soil: From theory to design. Blackie and Son Ltd., New York
2. Grossoni I, Powrie W, Zervos A, Bezin Y, Le Pen L Modelling railway ballasted track settlement in vehicle-track interaction analysis
3. Indraratna B et al (2006) Geotechnical properties of ballast and the role of geosynthetics in rail track stabilization. [Online]. Available https://ro.uow.edu.au/engpapers
4. Abadi T, Le Pen L, Zervos A, Powrie W (2018) Improving the performance of railway tracks through ballast interventions. Proc Inst Mech Eng F J Rail Rapid Transit 232(2):337–355. https://doi.org/10.1177/0954409716671545
5. Zhang X, Zhao C, Zhai W, Shi C, Feng Y (2019) Investigation of track settlement and ballast degradation in the high-speed railway using a full-scale laboratory test. Proc Inst Mech Eng F J Rail Rapid Transit, 233(8):869–881. https://doi.org/10.1177/0954409718812231
6. Aingaran S (2014) Experimental investigation and cyclic behaviour of scaled railway ballast and the effect of stress reversal. University of southampton, Southampton
7. Abadi T (2015) Effect of sleeper and ballast interventions on rail track performance
8. Le Pen LM, Powrie W (2011) Contribution of base, crib, and shoulder ballast to the lateral sliding resistance of railway track: A geotechnical perspective. In: Proceedings of the institution of mechanical engineers, Part F: Journal of Rail and Rapid Transit, pp 113–128. https://doi.org/10.1177/0954409710397094
9. Le Pen L, Bhandari AR, Powrie W (2014) Sleeper end resistance of ballasted railway tracks. J Geotech Geoenvironmental Eng, 140(5). https://doi.org/10.1061/(asce)gt.1943-5606.0001088
10. Lees G, Kennedy KC (1975) Quality, shape and degradation of aggregates. J Eng Geol
11. Chrismer SM (1986) Considerations of factors affecting ballast perfomance
12. Indraratna B, Ionescu D, Christie HD (1998) Shear behavior of railway ballast based on large-scale triaxial tests. J Geotech Geoenvironmental Eng, 124(5):439–449. https://doi.org/10.1061/(asce)1090-0241(1998)124:5(439)

13. Indraratna B, Asce F, Pramod, Thakur K, Vinod JS (2010) Experimental and numerical study of railway ballast behavior under cyclic loading. https://doi.org/10.1061/ASCEGM.1943-5622.0000055
14. Gupta A (2022) Mechanical properties of re-used ballast. University of Southampton, Southampton
15. Abadi T, Madhusudhan BN, Li H, Le Pen L (2023) Reusing life-expired railway ballast: laboratory testing, shape analysis, and petrographic evaluation. J Geotech Geoenvironmental Eng, 149(1). https://doi.org/10.1061/(asce)gt.1943-5606.0002904
16. Thakur PK, Vinod JS, Indraratna B (2014) Effect of particle breakage on cyclic densification of ballast: A DEM approach, In: IOP conference series: Materials science and engineering, Institute of Physics Publishing. https://doi.org/10.1088/1757-899X/10/1/012229
17. Burks ME, Robson JD, Shenton MJ (1975) Comparison of robel supermat and plasser 07–16 track maintenance machines. Tech. note TN SM 139, British Railways Board R & D Division
18. Wright SE (1983) Damage caused to ballast by mechanical maintenance techniques. British Rail Research Technical Memorandum
19. Aingaran S, Le Pen L, Zervos A, Powrie W (2018) Modelling the effects of trafficking and tamping on scaled railway ballast in triaxial tests. Transp Geotech 15(March):84–90. https://doi.org/10.1016/j.trgeo.2018.04.004
20. Salim W (2004) Deformation and degradation aspects of ballast and constitutive modelling Deformation and degradation aspects of ballast and constitutive modelling under cyclic loading under cyclic loading. University of Wollongong. [Online]. Available https://ro.uow.edu.au/theses
21. Indraratna B, Lackenby J, Christie D (2005) Effect of confining pressure on the degradation of ballast under cyclic loading. Géotechnique 55(4):325–328. https://doi.org/10.1680/geot.2005.55.4.325
22. Sun Y, Zheng C (2017) Breakage and shape analysis of ballast aggregates with different size distributions. Particuology 35:84–92. https://doi.org/10.1016/j.partic.2017.02.004
23. Powrie W, Le Pen L, Milne D, Thompson D (2019) Train loading effects in railway geotechnical engineering: Ground response, analysis, measurement and interpretation. Transp Geotech, 21(May):100261. https://doi.org/10.1016/j.trgeo.2019.100261
24. Fukushima S, Tatsuoka F (1984) Strength and deformation characteristics of saturated sand at extremely low pressures. Soils Found 24(4):30–48. https://doi.org/10.3208/sandf1972.24.4_30